

## Quantitative assessment of the local leakage current in PV modules for degradation prediction

H. Nagel, M. Glatthaar and S. W. Glunz

Fraunhofer Institute for Solar Energy Systems (ISE), Heidenhofstraße 2, 79110 Freiburg, Germany  
Email: henning.nagel@ise.fraunhofer.de

**ABSTRACT:** Small leakage currents flow between the frame and the active cell matrix in photovoltaic (PV) modules under normal operation conditions due to the not negligible electric conductivity of the module building materials. Even if the leakage current is well below the ground-fault detection threshold, predominantly the DC part can cause significant electrochemical corrosion of cell and frame metals, potential-induced degradation (PID) of the shunting type or PID of the solar cells' surface passivation. In general, it was found that the degradation rate has a high correlation with the leakage current density which is a strong function of position in large-area modules due to the voltage drop between the frame and the cells. In this work we measured material and surface conductivities and subsequently calculated the local leakage current density distribution in large-area PV modules in order to obtain quantitative insight into the local degradation. The shares of leakage currents through individual materials are discussed and, as an example, the width of the circumferential module area threatened by electrochemical corrosion was predicted under accelerated test conditions.

### 1 INTRODUCTION

The basic functions of photovoltaic (PV) module packaging are

- providing mechanically stable units which can be easily handled and durably fixed to mounting systems,
- protection of the solar cells against environmental impacts,
- electrical insulation of the active electrical elements to ensure human safety and
- building an assembly with increased electrical power output compared to single solar cells.

In order to realize d), usually a large number of cells are connected in series for the sake of voltage enhancement without current increase. In this way ohmic losses in the active cell matrix are kept low. A similar line of reasoning holds true for the series connection of single modules in PV systems. Therefore, in large installations the DC side system voltage is often as high as permitted by the module manufacturer. At this so-called maximum system voltage the module must be sufficiently well-insulated between current-carrying parts and the frame or the outside world. The corresponding tests are defined in the international standard IEC 61215 'design qualification and type approval'. Two tests, an insulation test and a wet leakage current test, are required. The first one is performed in air, the second during immersion of the module in a tank containing water featuring a resistivity  $< 3.5 \text{ k}\Omega \text{ cm}$ . In both tests the conductivity between the shorted output terminals and exposed metal parts of the module (e. g. the metal frame) is measured at room temperature. For modules larger than  $0.1 \text{ m}^2$  the pass criterion is that the conductivity divided by the module area shall not exceed  $2.5 \times 10^{-12} \text{ S/cm}^2$ .

Leakage currents flowing between the grounded mounting and the active cell matrix under normal operation conditions have to be kept low for reasons other than human safety as well. Predominantly the DC part of the leakage current can cause significant electrochemical corrosion of cell and frame metals, potential-induced degradation (PID) of the shunting type and PID of the solar cells' surface passivation [1,2,3]. In general, it was found that the degradation rate has a high correlation with the leakage

current density which is a strong function of position in large-area modules due to the voltage drop between the frame and the cells. Up to now in a few publications the local potential of the PV module surface was measured, see for example [4], but the local leakage current density distribution wasn't addressed. In order to get quantitative insight into local stress caused by leakage current, we measured bulk and surface conductivities of PV module building materials as a function of humidity and temperature in this study. From the obtained data we calculated the distribution of the local leakage current density through the front side of large-area PV modules. As an example of use we applied the results to the prediction of electrochemical corrosion of crystalline Si solar cells' front side metallization.

### 2 EXPERIMENT AND SIMULATION

We investigated i) the DC bulk conductivity of commercially available soda-lime glass commonly used for PV module manufacturing as a function of temperature, ii) the DC surface conductivity of the same soda-lime glass as a function of temperature and relative humidity (*RH*) and iii) the DC bulk conductivity of widespread ethylene vinyl acetate (EVA) encapsulation material as a function of temperature. The measurements were performed according to the IEC 60093 standard by means of a petaohmeter, a guard ring electrode and a counter electrode. In order to ensure good temperature and *RH* control, the contacted samples were placed in a climate chamber.

Measured surface and bulk conductivities were used to set up three-dimensional resistor networks representing large-area PV module structures. The resistor networks served as input data for numerical electronic circuit simulations by means of the software LTspice IV [5] that finally gave the local leakage current distributions.

### 3 RESULTS

#### 3.1 Electrical bulk and surface conductivity

The electrical conduction in soda-lime glasses is predominantly based on the transport of  $\text{Na}^+$  ions [6]. Ohm's law is valid at low and intermediate electric fields  $< 10^4 \text{ V/cm}$  [7] and at moderate temperatures the bulk conductivity  $\sigma$  is thermally activated according to Arrhenius law [8]. Our measurements agree very well with this behaviour and

with literature data on the bulk conductivity of soda-lime glass [9]. We found an activation energy  $E_a$  of 0.814 eV and a pre-exponential factor  $\sigma_0$  of 25.2 S/cm. Fig. 1 shows a plot of the sheet conductivity calculated from the measured bulk conductivity by multiplication with a glass thickness of 3.2 mm. This is a common thickness of crystalline Si PV modules' front cover glass. The reason why we plot the sheet conductivity of the cover glass (in S) instead of the bulk conductivity of the glass (in S/cm) is that the former allows for a direct quantitative comparison of lateral (i. e., parallel to the module surface) conduction in the module taking the different thicknesses of the layers into account. Note, that the conductivity of surfaces and interfaces featuring zero thickness can also be directly compared with the sheet conductivity of bulk layers.

Additionally, it is helpful to calculate the area-specific conductivity by dividing the glass bulk conductivity by the thickness of 3.2 mm, see Fig. 2. The area specific conductivity is relevant for current flowing perpendicularly to the module surface. Again, area specific conductivities can be directly compared.

The electrical bulk conductivity of EVA is also thermally activated and could therefore be fitted to Arrhenius

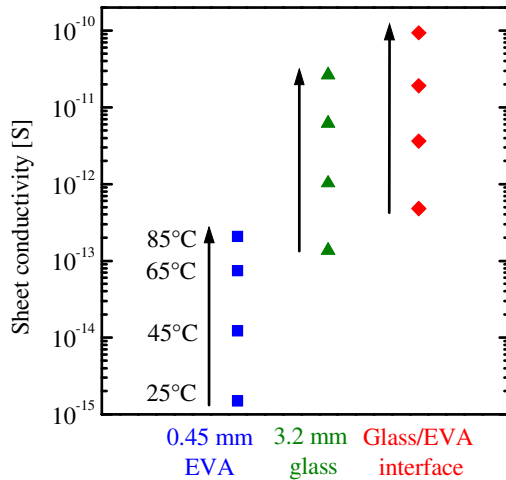


**Fig. 1:** Measured sheet conductivity of 0.45 mm thick EVA and 3.2 mm thick glass as a function of temperature. Additionally, the figure shows the conductivity of the glass/EVA interface deduced from [10] as a function of temperature.

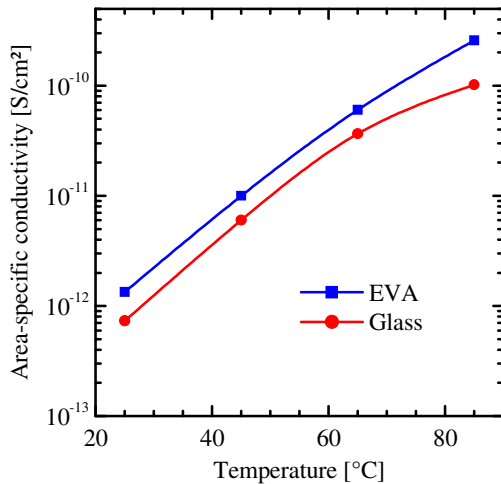


**Fig. 2:** Measured area-specific DC bulk conductivity of soda-lime glass and EVA as a function of temperature.

law. The obtained activation energy is 0.782 eV and the pre-exponential factor is 0.6 S/cm. Compared with the electrical bulk conductivity of EVA published in [1] our values are a factor of 4 to 6 higher. This quite large deviation is not surprising because in general the conductivity of EVA depends on the vinyl acetate concentration, the water content and the lamination parameters. The sheet and area-specific conductivities of the EVA layer were calculated using a common thickness in modules of 0.45 mm. It can be seen from Fig. 1 that the sheet conductivity of EVA is about two orders of magnitude lower compared with glass because it is thinner and its bulk conductivity is lower. Therefore, already at this point of time it becomes clear that the lateral current conduction through EVA is very low. In contrary, the area specific conductivity shown in Fig. 2 is a factor of about 2 higher compared with the glass cover because the EVA layer is very thin. Hence, the glass cover provides an important contribution for the electrical insulation perpendicular to the module's surface.

The measured surface conductivity of the front cover glass is depicted in Fig. 3 as function of temperature and relative humidity. It can be seen that it is thermally activated at a fixed RH. At a fixed temperature below a threshold  $RH_{th}$  it is nearly independent of RH. Beyond  $RH_{th}$  the surface conductivity heavily increases by up to more than one order of magnitude with growing RH depending on temperature. Interestingly,  $RH_{th}$  is to a first approximation independent of temperature and has a value of about 50 % for the investigated glass. In general, we expect that the surface conductivity and  $RH_{th}$  are both affected by the surface ion concentration, surface contaminants and weathering of the glass surface. Comparing the sheet conductivity of the glass surface with the one of the cover glass shown in Fig. 1 and Fig. 3 it can be seen that they are similar at high RH. At low RH the sheet conductivity of the cover glass is about one order of magnitude higher.

Another important current path through the PV module contributing to the front side leakage current is the current at the interface between front glass cover and EVA encapsulant which is labelled path 3 in Fig. 4. We didn't measure the conductivity of the glass/EVA interface in this study, but we deduced it from literature using our data. In [10] the leakage current through the EVA/soda-lime glass interface  $J_{1,3}$  was measured in comparison to the leakage current through 3.2 mm thick soda-lime glass ( $J_{1,2}$ , path 2 in Fig. 4). The ratio  $J_{1,3}/J_{1,2}$  averaged over a non-disclosed temperature and humidity cycle in the field was 2.9. Addi-

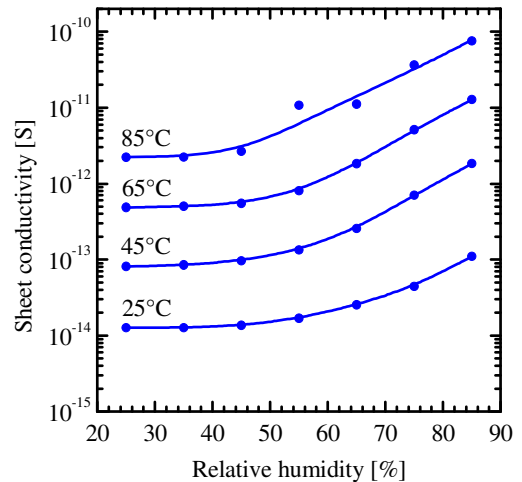


**Fig. 3:** Measured DC surface conductivity of soda-lime glass as a function of relative humidity and temperature.

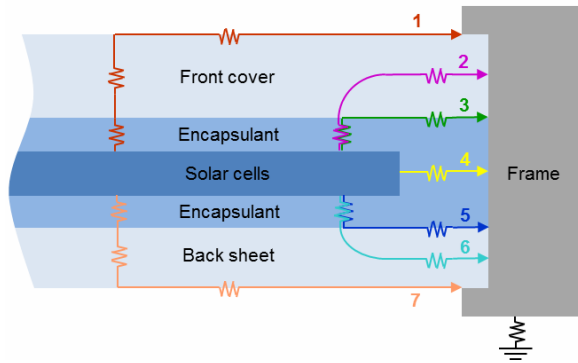


**Fig. 4:** Schematic drawing of a c-Si PV module cross section showing leakage current paths.

tionally, it was reported in [11] that the conductivity at the glass/EVA interface has similar temperature dependence as the bulk conductivity of the glass. Adopting this we get to the glass/EVA interface conductivity shown in Fig. 1 as a function of temperature. The values are consistent with the glass/EVA interface conductivity measured in [11] at 100 % RH. Because we expect that water in- and out-diffusion along the interface takes significant time, we argue that in the simulations presented in the next section the interface is saturated with water.

### 3.2 Electrical network simulations

There are 7 leakage current paths in crystalline Si PV modules, see schematic cross-sectional view in Fig. 4. From the data presented in Fig. 2 to Fig. 3 we calculated the leakage current densities along the paths 1 to 4 as a function of temperature and humidity for standard modules. In the simulations the voltage between cell matrix and circumferential module frame was set to 1000 V, a common maximum system voltage. Because the voltage between the electrical connectors of the module ( $\approx 0.55 \text{ V} \times 60 = 33 \text{ V}$ ; 60 being the number of c-Si cells in a module) is small compared to the voltage between cells and frame, we neglected the former. As mentioned before, the glass

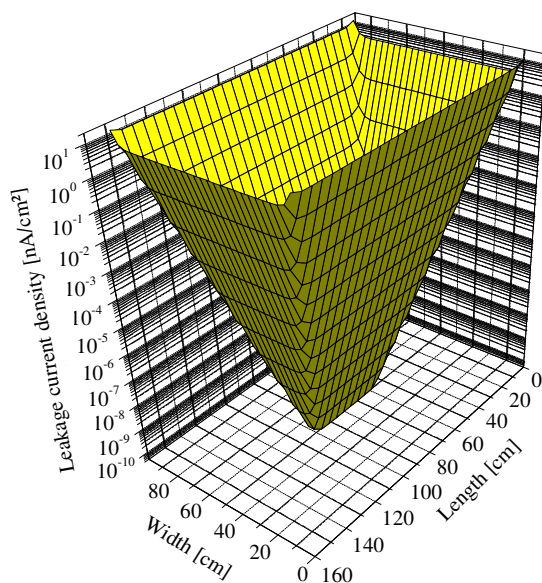


**Fig. 5 :** Three-dimensional representation of the calculated leakage current density through the front side of a standard large-area PV module at 85 °C, 85 % RH and 1000 V applied between active cell matrix and the circumferential metal frame.

thickness was set to 3.2 mm and the EVA encapsulation layer thickness was 0.45 mm. The outer dimensions of the modules were 99 x 160 cm².

Fig. 5 shows a three-dimensional plot of the front leakage current density obtained at a temperature of 85 °C and a relative humidity of 85 %. These are the damp heat test conditions defined in the standard IEC 61215. It can be seen from the figure that even under high temperature and high RH the local leakage current is extremely non-uniformly distributed in the module. Naturally the reasons are the low surface conductivity and the low sheet conductivity of the highly insulating materials in combination with large lateral module dimensions. In quantitative terms the leakage current density decreases by 12 orders of magnitude between frame and module center. For an easy comparison Fig. 6 shows two current density sections taken from Fig. 5 at a distance of 6.5 and 50 cm to the module edge in the short direction. Considering a distance between frame and outer cells of 2 cm, 6.5 cm distance to the frame means 4.5 cm distance to the outer edge of the cell matrix. It can be seen from the figure, that at this position the leakage current density exceeds a quite high value of 14 nA/cm².

The simulated local leakage current density is used to assess the local degradation caused by electrochemical corrosion of the cells' front metallization grid. In [12] a threshold charge density of about 0.1 C/cm² was given at which a solar cell power reduction of 25 % was observed. It has to be noted that among others the threshold charge density depends on the actual metallization stack, the encapsulation material and presumably also on temperature. Hence, the relevant value has to be measured for each specific combination of cell, module design and test condition. Here, the threshold charge density given in [12] serves to approximate the cell area in the module which is threatened by electrocorrosion after an assumed stress time of 0.5 years. The corresponding current density of 6 nA/cm² is marked by the dashed red line in Fig. 6. It can be seen, that 8 cm at the edge of the module face such a high stress that significant electrochemical corrosion can be expected.

In order to quantify the effect of humidity we performed a similar calculation at 25 % RH. The resultant leakage current density profiles are depicted in Fig. 7. At a distance of 6.5 cm to the frame the leakage current density exceeds 9.9 nA/cm². The width of the module edge threat-

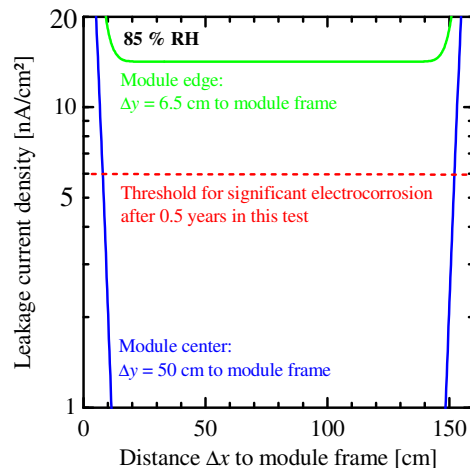


**Fig. 6:** Calculated leakage current density profiles at 85 °C, 85 % RH and 1000 V. The dotted red line shows the threshold leakage current density for electrocorrosion after a 0.5 years lasting test (according to [12]).

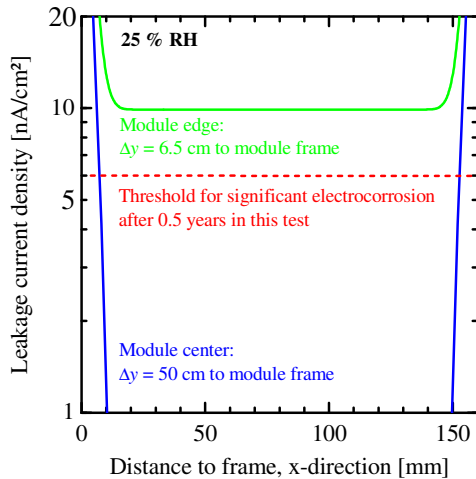


**Fig. 7:** Calculated leakage current density profiles at 85 °C, 25 % RH and 1000 V.

ened by electrocorrosion in a 0.5 years lasting stress test is reduced only marginally to 7.6 cm.

In this context it is interesting to look at the shares of the individual leakage current paths. Fig. 8 shows pie charts for all combinations of 25 °C, 85 °C, 25 % RH and 85 % RH. First of all it is striking that the share of the leakage current along the glass/EVA is dominating in every case. It amounts for about 76 % at 25 % RH and for 49 % to 66 % at 85 % RH. Hence, measures which reduce the sheet conductivity of this interface could effectively reduce the total leakage current.

Except at 85 °C / 85 % RH the second most important path is the lateral conduction through the glass cover. Its share lies between 19 % and 22 % at 25 °C / 25 %, 25 °C /

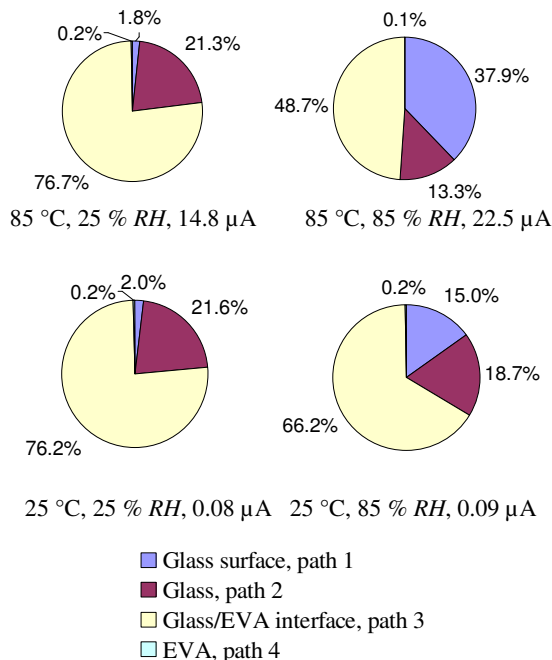


**Fig. 8:** Calculated shares of individual leakage currents through the front side of 100 x 160 cm<sup>2</sup> large PV modules. The corresponding current paths are depicted in Fig. 4. The temperature, relative humidity and the total leakage current obtained for 1000 V applied between cell matrix and frame are listed below the pie charts.

85 % and 85 °C / 25 %.

At 85 °C / 85 % the conduction along the glass surface has the second highest share of 38 %. At 25 °C / 85 % it accounts for 15 % of the total leakage current. At 25 % RH it is practically negligible, independent of temperature. It must be noted that in the field the conduction along the glass surface may heavily rise because of dirt and rain.

Finally, it can be seen in Fig. 8 that the contribution of the lateral current through the EVA is negligible at every investigated temperature and RH.

#### 4 SUMMARY

In order to assess the local leakage current density distribution in PV modules and the resulting possible local electrical power degradation we investigated the conductivity of common materials used for solar module construction, namely soda-lime glass and EVA. The bulk conductivities were measured as a function of temperature and the surface conductivity of the glass was measured as a function of temperature and relative humidity. Using the acquired data together with the temperature dependent conductivity of the interface between glass and EVA, which was deduced from literature, we simulated the local leakage current density through the front side of large-area PV modules at temperatures of 25 °C and 85 °C and at relative humidities of 25 % and 85 %. The most important results are:

- The leakage current along the glass/EVA is dominating for all temperatures and relative humidities.
- The second most important path is the lateral conduction through the glass except for 85 °C and 85 % RH.
- At a high RH of 85 % the conduction along the glass surface becomes important and accounts for up to 38 % of the total leakage current at 85 °C.
- The contribution of the lateral current through the EVA is negligible in any case.
- Even at a high temperature of 85 °C and a high relative humidity of 85 % and hence increased electrical conductivity the local leakage current density varies by about 12 orders of magnitude in 99 x 160 cm<sup>2</sup> large PV modules.

As an example of degradation prediction we calculated the area threatened by electrochemical corrosion after an accelerated test at 85 °C with 1000 V applied between the cell matrix and the module frame for 0.5 years. Irrespective of RH the width of the affected circumferential area is about 8 cm.

#### ACKNOWLEDGEMENT

The authors thank all former members of the solar cell and solar module development teams at SCHOTT Solar for their contributions and excellent co-operation. Part of this work was funded by the German Federal Ministry for Economic Affairs and Energy within the project ‚PID-s‘ under contract number 0325748A.

#### REFERENCES

- G. R. Mon and R. G. Ross, *Proceedings of the 18<sup>th</sup> IEEE PV Specialists Conference* (1985) 1142.
- J. Berghold, O. Frank, H. Hoehne, S. Pingel, B. Richardson and M. Winkler, *Proceedings of the 25<sup>th</sup> European Photovoltaic Solar Energy Conference*

- (2010) 3753.
- [3] R. Swanson, M. Cudzinovic, D. DeCeuster, V. Desai, J. Jürgens, N. Kaminar, W. Mulligan, L. Rodrigues-Barbosa, D. Rose, D. Smith, A. Terao, and K. Wilson, *Proceedings of the 15<sup>th</sup> International Photovoltaic Science & Engineering Conference* (2005) 410.
  - [4] Y. Hishikawa, K. Yamagoe and T. Onuma, *Jap. J. Appl. Phys.* 54 (2015) 08KG05.
  - [5] <http://www.linear.com/designtools/software/#LTspice>
  - [6] F. V. Natrup, H. Bracht, S. Murugavel and B. Roling, *Phys. Chem. Chem. Phys.* 7 (2005) 2279.
  - [7] R. J. Maurer, *J. Chem. Phys.* 9 (1941) 579.
  - [8] D. A. Stuart and O. L. Anderson, *J. Am. Ceram. Soc.* 36 (1953) 27.
  - [9] D. M. Robinson, *J. Appl. Phys.* 2 (1932) 52.
  - [10] N. G. Dhere, N. S. Shiradkar and E. Schneller, *Appl. Phys. Lett.* 104 (2014) 112103.
  - [11] G. R. Mon, L. Wen and R. Ross, *Proceedings of the 19<sup>th</sup> IEEE PV Specialists Conference* (1987) 1215.
  - [12] G. R. Mon, J. Orehotsky and R. G. Ross, *Proceedings of the 17<sup>th</sup> IEEE PV Specialists Conference* (1984) 682.